New insights into nitrous oxide emissions in a single-stage CANON process coupled with denitrification: thermodynamics and nitrogen transformation

Fang Fang, Kai Li, Jin-Song Guo, Han Wang, Ping Zhang and Peng Yan

ABSTRACT

The dynamic characteristics of N_2O emissions and nitrogen transformation in a sequencing batch biofilm reactor (SBBR) using the completely autotrophic nitrogen removal over nitrite (CANON) process coupled with denitrification were investigated via ^{15}N isotope tracing and thermodynamic analysis. The results indicate that the Gibbs free energy (ΔG) values of N_2O production by the nitrifier denitrification and heterotrophic denitrification reactions were greater than that of NH_2OH oxidation, indicating that N_2O was easier to produce via either nitrifier and heterotrophic denitrification than via NH_2OH oxidation. Ammonia-oxidizing bacteria (AOB) denitrification exhibited a higher f_s^0 (the fraction of electron-donor electrons utilized for cell synthesis) than NH_2OH oxidation. Therefore, AOB preferred the denitrification pathway because of its growth advantage when N_2O was produced by the AOB. The N_2O emissions by hydroxylamine oxidation, AOB denitrification and heterotrophic denitrification in the SBBRs using different C/N ratios account for 5.4–7.6%, 45.2–60.8% and 33.8–47.2% of the N_2O produced, respectively. The total N_2O emission with C/N ratios of 0, 0.67 and 1 was 228.04, 205.57 and 190.4 $\mu g\ N_2O\text{-}N \cdot g^{-1}$ VSS, respectively. The certain carbon sources aid in the reduction of N_2O emissions in the process.

Key words | CANON, denitrification, nitrogen transformation, N_2O emission, thermodynamics

HIGHLIGHTS

- N_2O emission was investigated in CANON coupled with denitrification (DN) process.
- ΔG values of AOB and heterotrophic DN were greater than that of NH_2OH oxidation.
- AOB was the primary contributor to N_2O emissions.
- The certain carbon sources aided in the reduction of N_2O emissions in the process.
- Restrained nitrifier DN by carbon source mainly caused the N_2O emissions reduction.

GRAPHICAL ABSTRACT

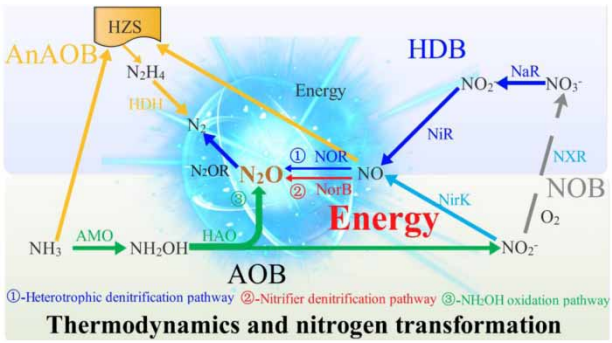

doi: 10.2166/wst.2020.344

Fang Fang
Jin-Song Guo
Peng Yan (corresponding author)
Key Laboratory of the Three Gorges Reservoir Region's Eco-Environment, Ministry of Education,
Chongqing University,
No.174, Shazhen Street, Chongqing 400045,
China
E-mail: *yanpengstu@163.com*

Kai Li
Han Wang
Ping Zhang
College of Eco-environment Engineering,
Guizhou Minzu University,
Huaxi District, Guiyang City, Guizhou 550025,
China

INTRODUCTION

In recent years, interest towards greenhouse gas (GHG) emission from wastewater treatment plants (WWTPs) has substantially increased, with the aim of minimizing their environmental impact (Mannina *et al.* 2018). Nitrous oxide (N_2O) is an important GHG with a high global warming potential (approximately 298 times higher than that of CO_2) (Desloover *et al.* 2012). In general, the autotrophic nitrogen removal processes in WWTPs are considered a major source of N_2O (Spinelli *et al.* 2018). The completely autotrophic nitrogen removal over nitrite (CANON) process is an energy saving and cost-effective biological nitrogen removal process because of its reduced carbon source and oxygen demands and decreased sludge production (Sliekers *et al.* 2002). Currently, the CANON process coupled with denitrification has been widely employed to treat high ammonium-contained wastewater with a low C/N ratio (Lackner *et al.* 2014). Excellent nitrogen removal can be achieved using the CANON process coupled with denitrification, which has been demonstrated as an economically feasible option for practical applications (Vázquez-Padín *et al.* 2009). However, N_2O emission from this process decreases evidently its own the environmental sustainability (Connan *et al.* 2018).

A better understanding of the mechanism of N_2O production would help facilitate the development of generic mitigation strategies for reducing N_2O emissions resulting from the CANON process coupled with denitrification. The following three primary microbial pathways are involved in the N_2O production in this process: the hydroxylamine (NH_2OH) oxidation pathway, the nitrifier denitrification pathway and the heterotrophic denitrification pathway. Although N_2O production pathways have been extensively investigated in a large amount of previous studies, there is still controversy concerning the mechanism of N_2O production (Domingo-Félez & Smets 2019). Often, various N_2O production pathways simultaneously occur, and each pathway is differently regulated by a variety of environmental factors (Law *et al.* 2011; Rathnayake *et al.* 2013). Therefore, determining the relative contributions of each pathway to total N_2O production remains challenging because of the lack of effective methodologies and analytical tools needed for the identification and characterization of N_2O production. This issue has led to different studies reporting contradictory observations (Duan *et al.* 2017; Ma *et al.* 2017). Therefore, effective methodologies and analytical tools for characterizing different production pathways and their effects on the total N_2O emissions are still needed to develop targeted strategies for controlling and reducing N_2O emissions.

The essence of microbial nitrogen metabolism is material- and energy transformation-based nitrogen metabolism (Rittmann & McCarty 2012). Biochemical reactions in nitrogen metabolism are accompanied by material recombination and energy changes. Therefore, thermodynamics and material tracing can be effectively used to elucidate the synthetic pathway and mechanism of nitrogen-based products involved in nitrogen metabolism. The objective of this study was to accurately identify N_2O production pathways and their contributions to the total N_2O emissions by a quantitative analysis approach based on ^{15}N isotope tracing. Additionally, the dynamic characteristics of N_2O emissions and nitrogen transformation in a sequencing batch biofilm reactor (SBBR) using the CANON process coupled with denitrification were investigated based on a thermodynamic model and stoichiometry. The results of this study provided a better understanding of N_2O production and important information concerning the N_2O emissions reduction from the CANON process coupled with denitrification.

MATERIALS AND METHODS

Wastewater characteristics and reactor operation

Three different types of wastewater with different C/N ratios (0.00, 0.67 and 1.00; Table S1 in Supplementary Information) were fed simultaneously into three identical SBBR reactors in parallel. The effective volume of each SBBR was 30 L (9 L of flexible medium for biofilm growth, 30% (V/V); Figure S1). The SBBR was operated under intermittent aeration (non-aeration: aeration $n =$ 2 h:2 h) with a hydraulic retention time (HRT) of 48 h. The reactor temperature was maintained at 30 ± 1 °C with a cycle time of 24 h (4 min of feeding, 23 h of reaction, 30 min of settling and 26 min of decanting). The dissolved oxygen (DO) in the aeration phase ranged from 1.5 to 2.0 mg L^{-1} and was controlled using a DO controller and probe (Bell, BDO-200D, China). During each cycle, 10.5 L of the supernatant was decanted from the SBBR, and then an equal volume of wastewater was fed into the reactor at the beginning of the next cycle.

The operation of the reactor and process parameters used in this study were reported in Yan *et al.* (2019).

Batch experiments

Isotopic tracer experiments

Three 0.5-L sealed bottles (A, B and C) each contained 150 g fresh biofilm from the SBBRs with different C/N ratios (Figure S2). An identical sealed bottle (D) without biofilm served as a control. A 350-mL sample of different types of wastewater containing a ^{15}N-$NaNO_2$ isotopic tracer (Table S2) was added into each bottle. The off-gas was collected to determine the isotopic compositions of N_2O and N_2. Synchronously, 2-mL liquid samples were collected to analyze the concentrations of NH_4^+-N, NO_2^--N, NO_3^--N and total nitrogen (TN). The isotopic tracer protocol used in this study was originally described in Li *et al.* (2017). Each sample was analyzed three times.

Inhibition experiments

The co-use of allylthiourea (ATU) and $NaClO_3$ effectively inhibits the N_2O production via ammonia-oxidizing bacteria (AOB) denitrification (Tallec *et al.* 2008), whereas N_2O emissions by heterotrophic bacteria are not significantly affected by specific chemical inhibitors. Therefore, N_2O emissions produced by heterotrophic denitrifying (HD) bacteria alone and by both AOB and heterotrophic denitrification can be determined quantitatively by batch experiments conducted either with or without inhibitors. The following three batch experiments were conducted: (I) without nitrite or inhibitor, (II) with nitrite and (III) with both ATU and $NaClO_3$. The inhibition experiments used herein were originally described in Li *et al.* (2017).

Analysis

The NH_4^+-N, NO_2^--N, NO_3^--N and TN concentrations were determined by a flow injection analyzer (Hach Quickchem 8500S2, Hach Inc., USA). N_2O concentration was measured using a gas chromatograph (Agilent 7820A, Agilent Technology Inc., USA). The isotopic compositions of N_2O and N_2 were analyzed via gas chromatography-isotope ratio mass spectrometry (Delta V advantage, Thermo Electron, Germany) and used to calculate the accumulation of ^{15}N-labeled N_2O as $^{45}N_2O$ ($^{14}N^{15}N^{16}O$) and $^{46}N_2O$ ($^{15}N^{15}N^{16}O$) and N_2 as $^{29}N_2$ ($^{14}N^{15}N$) and $^{30}N_2$ ($^{15}N^{15}N$). The isotopomer analysis method used herein was originally described in Li *et al.* (2017).

Microbial community analysis

Fresh biofilm samples were collected and then immediately placed in storage at −20 °C. Sequencing using an Illumina MiSeq PE300 sequencing platform was performed by Majorbio Bio-Pharm Technology Co., Ltd. Primers 338F and 806R were used to amplify the V3-V4 regions of the bacterial 16S rDNA genes from the extracted DNA. The gene pyrosequencing methods used herein were originally reported in Wang *et al.* (2017).

Fluorescence *in situ* hybridization (FISH)

Thin sections of biofilms were mounted on Teflon-coated glass slides. Hybridization was performed using hybridization probes NSO1225, GAM42a-T1038 (Pxyn-440) and AMX820 to identify AOB, HD and Anaerobic Ammonium Oxidation (anammox) bacterial populations, respectively. The probes were labeled with fluorescein isothiocyanate (FITC), Cy5 and Cy3 at the 5′ end. Hybridized samples were observed with a LSM700 confocal laser-scanning microscope equipped with three diode lasers (488, 555 and 639 nm; Carl Zeiss, Oberkochen, Germany). The fluorescent *in situ* hybridization (FISH analysis) method used herein was originally reported in Ali *et al.* (2016).

Nitrogen removal pathway

NO_2^- was labeled with ^{15}N and NH_4^+-N was not labeled in isotopic tracer experiments (Li *et al.* 2017). $^{28}N_2$ and $^{29}N_2$ were produced by anammox in the batch experiment system used herein. Equations (1) and (2) were obtained by balancing atomic numbers:

$$a_{28} = (1 - F) \cdot a_{N_2} \quad (1)$$

$$a_{29} = F \cdot a_{N_2} \quad (2)$$

where a_{N_2} represents the total production of N_2 by anammox; a_{28} and a_{29} represent the production of $^{28}N_2$ and $^{29}N_2$ by anammox, respectively; and F represents the ^{15}N abundance of $^{14/15}NaNO_2$ in the batch experiment system.

$^{28}N_2$, $^{29}N_2$ and $^{30}N_2$ were produced by heterotrophic denitrification in the batch experiment system, and they comprised $(1 - F)^2$, $2{\cdot}F{\cdot}(1 - F)$ and F^2, respectively, of the total production of N_2 by heterotrophic denitrification.

Equations (3)–(5) were then obtained:

$$d_{28} = (1-F)^2 \cdot d_{N_2} \quad (3)$$

$$d_{29} = 2F(1-F)d_{N_2} \quad (4)$$

$$d_{30} = F^2 \cdot d_{N_2} \quad (5)$$

where d_{N_2} represents the total production of N_2 by heterotrophic denitrification and d_{28}, d_{29} and d_{30} represent the production of $^{28}N_2$, $^{29}N_2$ and $^{30}N_2$ by heterotrophic denitrification, respectively.

Equations (6)–(8) were obtained using the gas mass balance:

$$T_{28} = a_{28} + d_{28} \quad (6)$$

$$T_{29} = a_{29} + d_{29} \quad (7)$$

$$T_{30} = d_{30} \quad (8)$$

where T_{28}, T_{29} and T_{30} represent the generation of $^{28}N_2$, $^{29}N_2$ and $^{30}N_2$, respectively, in the batch experiment system. These gases were directly measured by GC-IRMS.

Equation (9) was obtained by soing Equations (5) and (8) simultaneously:

$$d_{N_2} = T_{30} \cdot F^{-2} \quad (9)$$

Equation (10) was obtained by solving Equations (2), (4), (7) and (9) simultaneously:

$$a_{N_2} = F^{-1} \cdot T_{29} + 2(1-F^{-1}) \cdot T_{30} \quad (10)$$

The contributions of heterotrophic denitrification (C_d) and anammox (C_a) to TN removal were calculated by Equations (11) and (12), respectively:

$$\mathrm{C_d} = \frac{1}{\mathrm{F} \cdot (T_{30}/T_{29} + 2) - 1} \cdot 100\% \quad (11)$$

$$C_a = (1 - C_d) \cdot 100\% \quad (12)$$

Calculation of N_2O emissions

N_2O emissions from nitritation and denitrification were calculated using Equations (1)–(7), which were based on the ^{15}N mass balance. The N_2O emissions produced by denitrification (II-I) were further identified as the contributions from nitrifier denitrification (II-III) and HD bacteria (III-I) by Equations (13) and (14), respectively (Fig. S3).

$$M_{ND} = M_{II} - M_{III} \quad (13)$$

$$M_{HD} = M_{III} - M_I \quad (14)$$

where M_I, M_{II} and M_{III} represent the N_2O production in the collected sample from batch experiments I, II and III, respectively, and M_{ND} and M_{HD} represent the N_2O emissions from nitrifier denitrification and HD bacteria.

Thermodynamic model and stoichiometry

During the CANON process coupled with denitrification, a portion of the electrons (f_e^0, eeq cells/eeq donor) in the electron donors (substrates) are transmitted to the terminal electron acceptor with energy generation. The remaining electrons in the electron donors (f_s^0, eeq cells/eeq donor) are utilized for cell synthesis. The electron allocation between energy generation and cell synthesis obeys the electron conservation laws Equation (15).

$$f_s^0 + f_e^0 = 1 \quad (15)$$

McCarty established a thermodynamic electron equivalents model to evaluate the microbial yield (McCarty 2007). A schematic diagram of the model is shown in Fig. S4. This model can regulate between energy reactions (R_e) and cell synthesis reactions (R_s):

$$f_s^0 = \frac{\Delta G_r}{\Delta G_r - \Delta G_s/\varepsilon} \quad (16)$$

$$\Delta G_r = \Delta G_a - \Delta G_d - \frac{q}{p}\Delta G_{xy} \quad (17)$$

$$\Delta G_s = \frac{(\Delta G_{fa} - \Delta G_d)}{\varepsilon^m} + \frac{(\Delta G_{in} - \Delta G_{fa})}{\varepsilon^n} + \frac{\Delta G_{pc}}{\varepsilon} \quad (18)$$

where ΔG_a (kJ/eeq) and ΔG_d (kJ/eeq) represent the reduction potentials for electron acceptor and electron donor half-reactions, respectively; ΔG_s (kJ/eeq) and ΔG_r (kJ/eeq) represent the Gibbs free energy for cell synthesis reactions and energy reactions, respectively; ΔG_{xy} and ΔG_{in} represent the reduction potentials of NADH oxidation (219.2 kJ/mol) and the acetyl-CoA half-reaction (30.9 kJ/eeq), respectively; ΔG_{fa} represents the reduction potentials of the formaldehyde half-reaction (46.53 kJ/eeq for single-carbon compounds; 0 kJ/eeq for all other compounds);

and ΔG_{pc} represents the Gibbs free energy (ΔG) of the intermediate conversion to cells (18.8 kJ/eeq when ammonia was used as the nitrogen source and for a cell chemical formula of $C_5H_7O_2N$). When the nitrogen source was N_2, nitrite or nitrate, pcells (per mole of cells) was 23, 26 or 28 kJ/eeq, respectively.). In addition, ϵ represents the energy transfer efficiency (0.6 in aerobic bacteria and 0.4 in anoxic bacteria); $m = +1$ if $\Delta G_{fa} > 0$, otherwise $= n$; $n = +1$ if $m = n$ and $(\Delta G_{in} - \Delta G_d) > 0$, otherwise $n = -1$; p represents the number of electron equivalents per mole of substrate from the half-reaction reduction equation; and q represents the number of oxygenase reactions per mole of substrate.

The biological processes can be described by combining the half-reactions and the calculated values for f_e^0 and f_s^0 Equation (19):

$$R = f_s^0 R_c + f_e^0 R_a - R_d \tag{19}$$

where R_c, R_a, and R_d represent the half-reactions for the microbial biomass synthesis, electron acceptor, and electron donor, respectively; and R represents the overall balanced reaction;

The ΔG for the overall balanced reaction (R) was calculated using the free energies of formation for various chemical species within the balanced biochemical equations using Equation (20):

$$\Delta G = \sum_{i=1}^{i=n} (v_i \Delta G_i^0)_P - \sum_{i=1}^{i=n} (v_i \Delta G_i^0)_R \tag{20}$$

where v_i is the stoichiometric coefficient of i in the reaction and ΔG_i is the free energy of formation. Using these data and Equation (20), ΔG was calculated for each equation.

Details about the computational procedures about the ΔG for the overall balanced reaction are provided in the Supplementary Information.

RESULTS AND DISCUSSION

Nitrogen removal performance in SBBRs

The nitrogen removal rates in the SBBRs with C/N ratios of 0, 0.67 and 1.00 were 81.4, 82.3 and 84.1%, respectively (Figure 1(a)–1(c)). The nitrogen removal reported in previous studies using the CANON process coupled with denitrification was 70–84% (Chen *et al.* 2009; Liang *et al.* 2014; Zhang *et al.* 2017). Excellent nitrogen removal was observed in the three SBBRs studied herein. The nitrogen removal rates increased from 81.4 to 84.1% when the C/N ratio increased from 0 to 1, indicating the carbon source increased nitrogen removal in the process. Nitrogen removal was improved using enhanced heterotrophic denitrification via addition of a carbon source. These results were in agreement with those of Zhang *et al.* (2017). Anammox and heterotrophic denitrification are the main nitrogen removal pathways present in the process. The contributions of the two pathways to TN removal with different C/N ratios are presented in Figure 1(d). Anammox was the primary nitrogen removal pathway in the process, and the contribution of anammox to TN removal was greater than 72%. The contribution of heterotrophic denitrification to TN removal increased from 10 to 28% as the C/N ratio increased from 0 to 1, indicating the carbon source significantly affected the contributions of heterotrophic denitrification and anammox to the TN removal of the process.

Prediction of N_2O emission potential based on thermodynamics

The transformation of N to N_2O is closely related to the nitrite production and consumption of the CANON process (Okabe *et al.* 2011; Yan *et al.* 2019). Nitrite production or consumption was regarded as an endpoint or starting point for the thermodynamic calculations used for the three N_2O emission pathways, NH_2OH oxidation, nitrifier denitrification and heterotrophic denitrification (described in Supplementary Information). The half-reactions and overall reactions of the different N_2O production pathways are shown in Tables 1 and 2. Bacterial growth and intracellular substance synthesis depends on the substrate allocation between catabolism and anabolism. f_s^0 represents the substrate used for cell synthesis. A higher f_s^0 is beneficial for the synthesis and growth of bacteria (Rittmann & McCarty 2012). The f_s^0 values for the NH_2OH oxidation, nitrifier denitrification and heterotrophic denitrification pathways were 0.28, 0.56 and 0.70, respectively. N_2O was produced by AOB via NH_2OH oxidation and denitrification. AOB denitrification exhibited a higher f_s^0 with regard to substrate allocation than NH_2OH oxidation. The value of f_s^0 in nitrifier denitrification was two-fold that of the NH_2OH oxidation. Therefore, AOB preferred the denitrification pathway because of its growth advantage when N_2O was produced by the AOB. The energy reaction is intended to provide the energy for microbial synthesis, which is a key step for the survival of microorganisms. The $\Delta G_e{}^0$ values

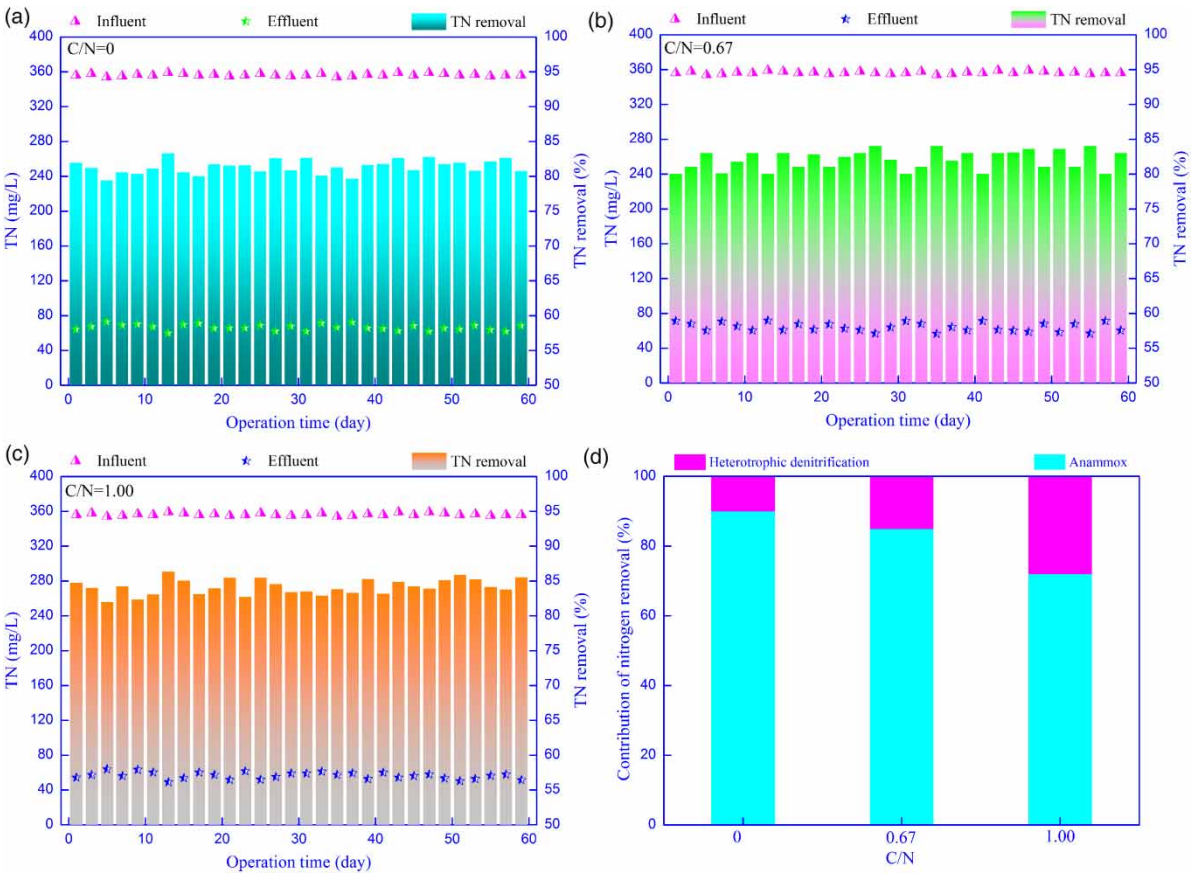

Figure 1 | Nitrogen removal at C/N ratios of 0 (a), 0.67 (b) and 1.00 (c) in SBBRs, and contributions of anammox and heterotrophic denitrification to TN removal (d).

Table 1 | Theoretical substrates allocation and half reaction of the different N_2O production pathway

N_2O production pathway	Half reaction	ΔG^0 (kJ/eeq)	f_s^0	f_e^0	ΔG_e^0 (kJ/eeq)	ΔG_s^0 (kJ/eeq)
NH_2OH oxidation	$\frac{1}{4}O_2 + H^+ + e^- \rightarrow \frac{1}{2}H_2O$ (R_a)	−78.14	0.28	0.72	−43.99	29.00
	$\frac{1}{8}N_2O + \frac{5}{4}H^+ + e^- \rightarrow \frac{1}{4}NH_4^+ + \frac{1}{8}H_2O$ (R_d)	−12.68				
	$\frac{1}{5}CO_2 + \frac{1}{20}HCO_3^- + \frac{1}{20}NH_4^+ + H^+ + e^- \rightarrow \frac{1}{20}C_5H_7O_2N + \frac{9}{20}H_2O$ (R_c)	103.57				
Nitrifier denitrification	$\frac{1}{2}NO_2^- + \frac{3}{2}H^+ + e^- \rightarrow \frac{1}{4}N_2O + \frac{3}{4}H_2O$ (R_a)	−230.35	0.56	0.44	−90.71	56.42
	$\frac{1}{4}NO_2^- + \frac{5}{4}H^+ + e^- \rightarrow \frac{1}{4}NH_2OH + \frac{1}{4}H_2O$ (R_d)	−10.64				
	$\frac{1}{5}CO_2 + \frac{1}{20}HCO_3^- + \frac{1}{20}NH_4^+ + H^+ + e^- \rightarrow \frac{1}{20}C_5H_7O_2N + \frac{9}{20}H_2O$ (R_c)	103.57				
Heterotrophic denitrification	$\frac{1}{2}NO_2^- + \frac{3}{2}H^+ + e^- \rightarrow \frac{1}{4}N_2O + \frac{3}{4}H_2O$ (R_a)	−230.35	0.70	0.30	−100.90	32.64
	$\frac{9}{50}CO_2 + \frac{1}{50}NH_4^+ + \frac{1}{50}CO_3^- + H^+ + e^-$ (R_h) $\rightarrow \frac{1}{50}C_{10}H_{19}O_3N + \frac{9}{25}H_2O$ (R_d)	380				
	$\frac{1}{5}CO_2 + \frac{1}{20}HCO_3^- \frac{1}{20} + NH_4^+ + H^+ + e^- \rightarrow \frac{1}{20}C_5H_7O_2N + \frac{9}{20}H_2O$ (R_c)	103.57				

pH is 7, and the temperature is 25 °C.

Table 2 | Overall reaction of the different N_2O production pathway

N_2O production pathway	Overall reaction	ΔG^0 (kJ/eeq)
NH_2OH oxidation	$\frac{9}{50}O_2+\frac{7}{125}CO_2+\frac{7}{500}HCO_3^-+\frac{33}{125}.NH_4^+=\frac{7}{500}C_5H_7O_2N+\frac{1}{8}N_2O+\frac{1}{4}H^++\frac{361}{1000}H_2O$	−14.99
Nitrifier denitrification	$\frac{14}{125}CO_2+\frac{7}{250}HCO_3^-+\frac{7}{250}NH_4^++\frac{1}{4}NH_2OH=\frac{7}{250}C_5H_7O_2N+\frac{11}{100}N_2O+\frac{3}{100}NO_2^-+\frac{88}{250}H_2O+\frac{3}{100}H^+$	−34.29
Heterotrophic denitrification	$\frac{1}{50}C_{10}H_{19}O_3N+\frac{3}{20}NO_2^-+\frac{3}{20}H^++\frac{3}{200}HCO_3^-+\frac{3}{200}NH_4^+=\frac{7}{200}C_5H_7O_2N+\frac{1}{25}CO_2+\frac{9}{50}H_2O+\frac{3}{40}N_2O$	−68.26

Domestic sewage ($C_{10}H_{19}O_3N$) is electron donors. The cell formulation is $C_5H_7O_2N$.

for the observed energy reactions ($f_e^0R_a - R_d$) of the NH_2OH oxidation, nitrifier denitrification and heterotrophic denitrification pathways were −43.99 kJ/eeq, −90.71 kJ/eeq and −100.90 kJ/eeq, respectively (Table 2), indicating that the energy reactions were thermodynamically favorable. The released energy can be used for microbial metabolism. The energy released by nitrifier denitrification and heterotrophic denitrification was significantly higher than that released by the NH_2OH oxidation. The $\Delta G_s{}^0$ values for the observed synthesis reactions ($f_s^0R_c$) of the NH_2OH oxidation, nitrifier denitrification and heterotrophic denitrification pathways were 29.00 kJ/eeq, 56.42 kJ/eeq and 32.64 kJ/eeq respectively (Table 2), indicating that the synthesis reactions were not spontaneous. The energy released by the energy reactions was needed to drive the synthesis reactions of the NH_2OH oxidation, nitrifier denitrification and heterotrophic denitrification pathways. However, the ΔG values for the overall reactions of the NH_2OH oxidation, nitrifier denitrification and heterotrophic denitrification pathways were −14.99 kJ/eeq, −34.29 kJ/eeq and −68.26 kJ/eeq, respectively, indicating the overall reactions were thermodynamically favorable. The ΔG value of N_2O production by nitrifier denitrification was more than twice that of the NH_2OH oxidation, indicating that the N_2O was more easily produced by nitrifier denitrification. The nitrifier denitrification is a main pathway of N_2O emissions by AOB. This result was consistent with the result of Wrage *et al.* (2001). The ΔG values of the nitrifier denitrification and heterotrophic denitrification reactions were greater than that of the NH_2OH oxidation. Therefore, N_2O was easier to produce using either nitrifier and heterotrophic denitrification than using NH_2OH oxidation. A lower energy release by the energy reactions was a limiting factor for the production of N_2O by the NH_2OH oxidation pathway. Therefore, from a thermodynamic perspective, the N_2O production by denitrification (nitrifier and denitrifier) was the main factor that contributed to the N_2O emissions.

N_2O emissions via nitrification and denitrification with different C/N ratios

The nitrification and denitrification emission characteristics of N_2O during batch experiments are shown in Figure 2. The N_2O was primarily generated during the first half of the batch experiments (0–6 h) (Figure 2(a) and 2(b)). N_2O production during the first 6 h of operation when C/N ratios of 0, 0.67 and 1 were used accounted for 72.4, 72.5 and 70.6%, respectively, of the total N_2O production. The N_2O production rates obtained with different C/N ratios increased over the first 3 h of the batch experiments; subsequently, they decreased significantly as the reaction progressed. The denitrification N_2O production rates when C/N ratios of 0, 0.67 and 1 were used increased from 22.27, 22.50 and 16.45 μg N_2O-N·g^{-1} VSS·h^{-1} to 30.37, 26.62 and 24.62 μg N_2O-N·g^{-1}VSS·h^{-1}, respectively, during the first 3 h of the batch experiments and then gradually decreased to 4.91, 4.09 and 7.54 μg N_2O-N·g^{-1} VSS·h^{-1}. Similar changes in the nitrification N_2O production rates were observed in batch experiments with different C/N ratios. The average denitrification N_2O production rates were 17.00, 15.12 and 13.97 μg N_2O-N·g^{-1} VSS·h^{-1}, respectively. The average denitrification N_2O production rates decreased as the C/N ratio increased. The results indicated that the addition of certain carbon sources inhibits N_2O emissions produced by denitrification in the process. The average N_2O production rates by nitrification using C/N ratios of 0, 0.67 and 1 were 0.92, 1.16 and 0.95 μg N_2O-N·g^{-1} VSS·h^{-1}, respectively. The carbon source had no

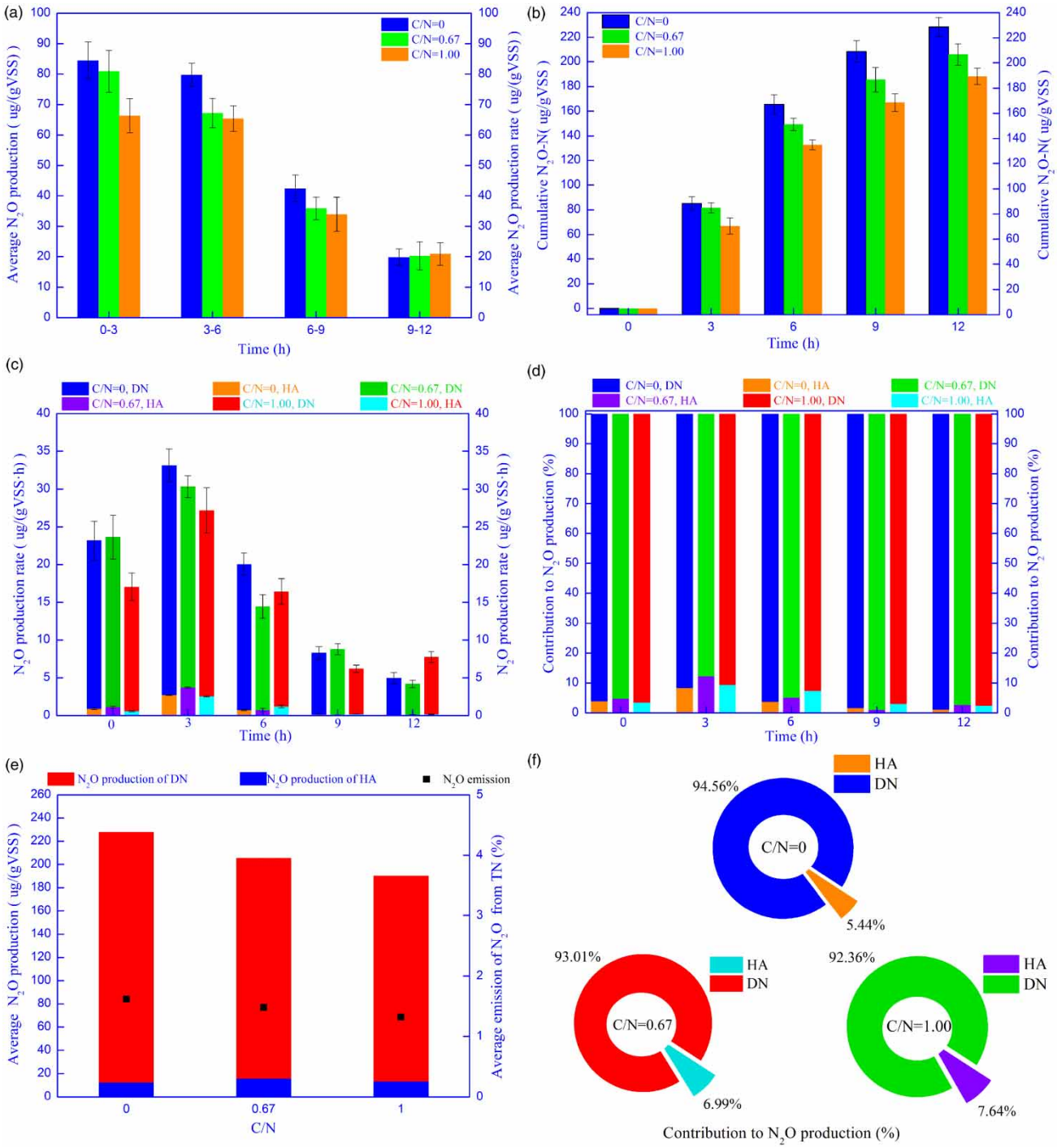

Figure 2 | Nitrification and denitrification N_2O emission characteristics during batch experiments with different C/N ratios: average N_2O production rate at each time interval (a), cumulative N_2O emissions (b), variation in N_2O production rate via nitrification and denitrification over time (c), variation in contributions of nitrification and denitrification to total N_2O production over time (d), average N_2O production and conversion rate of N_2O from TN (e) and average contribution of nitrification and denitrification to the total N_2O production (f).

significant effect on N_2O emission by nitrification in the process. In addition, the average denitrification N_2O production rates when different C/N ratios were used were far greater than the average nitrification rates, indicating denitrification was the primary N_2O emission source in the CANON process coupled with denitrification (Figure 2(d)).

The total N_2O production with C/N ratios of 0, 0.67 and 1 was 228.04, 205.57 and 190.4 μg N_2O-N·g^{-1} VSS, respectively. These results indicated that certain carbon sources aid in the reduction of N_2O emissions in this process. Decreased N_2O production using denitrification was the primary contributor to reducing N_2O emissions in this study. N_2O emissions from TN with C/N ratios of 0, 0.67 and 1 were 1.62, 1.48 and 1.32%, respectively. N_2O emissions from TN ranged from 1.2 to 2% in previous studies using partial nitritation/anammox (Kampschreur *et al.* 2009; Weissenbacher *et al.* 2010; Castro-Barros *et al.* 2015). The contributions of nitrification to the total N_2O generation with C/N ratios of 0, 0.67 and 1 were 5.44, 6.99 and 7.64%, respectively. The contributions of denitrification to the total N_2O production were 94.56, 93.01 and 92.36%, respectively. The carbon source produced a significant effect on the contributions of denitrification and nitrification with regard to the total N_2O production of the CANON process coupled with denitrification, which led to a decreasing trend in N_2O production by denitrification as the C/N ratio increased.

N_2O emissions via nitrifier and heterotrophic denitrification

The nitrogen transformation and emission characteristics of N_2O via nitrifier and heterotrophic nitrification during the inhibition experiments with different C/N ratios are presented in Figure 3. The nitrogen transformation and removal performance characteristics are shown in Figure 3(a)–3(c). The NO_2^--N removal rate obtained in inhibition experiment II using different C/N ratios was significantly higher than that obtained in inhibition experiment III, indicating inhibitors significantly affected AOB denitrification. The NO_3^--N production rate obtained in inhibition experiment II was lower than that obtained in inhibition experiment III because of the inhibition of nitrite reductase (NiR) activity by $NaClO_3$. The TN removal rate decreased after the addition of inhibitors with different C/N ratios, indicating AOB denitrification contributes to TN removal. The TN removal rates obtained in inhibition experiment II when C/N ratios of 0, 0.67 and 1 were used were 0.41, 0.43 and 0.45 mg N·g^{-1}·VSS·h^{-1}, respectively. The TN removal rate obtained in inhibition experiment II increased by 9% as the C/N ratio increased, indicating the presence of a carbon source promotes denitrification. The TN removal rates obtained in inhibition experiment III with C/N ratios of 0, 0.67 and 1 were 0.32, 0.35 and 0.39 mg N·g^{-1}·VSS·h^{-1}, respectively. The TN removal rate increased by 22.0% as the C/N ratio increased. These results indicated that heterotrophic denitrification is more sensitive to carbon source and that the increased heterotrophic denitrification is the main factor that contributes to the increase in the TN removal rate.

The N_2O production by denitrification decreased gradually with increasing C/N ratio. The N_2O production by nitrifier denitrification with C/N ratios of 0, 0.67 and 1 was 134.04, 78.64 and 80.16 μg N_2O-N·g^{-1} VSS, respectively. The N_2O production by heterotrophic denitrification with C/N ratios of 0, 0.67 and 1 was 76.64, 84.72 and 80.97 μg N_2O-N·g^{-1} VSS, respectively. These results indicated the addition of a carbon source reduced N_2O production by nitrifier denitrification; however, it had no significant impact on N_2O production via heterotrophic denitrification. The N_2O emissions from TN with C/N ratios of 0, 0.67 and 1 were 1.52, 1.28 and 1.11%, respectively. The contributions of nitrifier denitrification to the total N_2O production with C/N ratios of 0, 0.67 and 1 were 63.62, 48.14 and 49.75%, respectively. The contributions of heterotrophic denitrification to the total N_2O production with C/N ratios of 0, 0.67 and 1 were 36.38, 51.86 and 50.25%, respectively. The decreased nitrifier denitrification was the primary contributor to the decrease in N_2O production via denitrification. Therefore, based on the results presented in the section N_2O emissions via nitrification and denitrification with different C/N ratios, the decreased nitrifier denitrification resulting from the addition of a carbon source caused a decrease in the total N_2O emissions of the process.

N_2O emissions and mitigation

The compositions of N_2O emissions in the SBBRs using different C/N ratios are shown in Figure 4(a). The N_2O emissions by hydroxylamine oxidation, AOB denitrification and heterotrophic denitrification in the SBBRs using different C/N ratios account for 5.4–7.6%, 45.2–60.8% and 33.8–47.2% of the N_2O produced, respectively. The results indicated AOB denitrification and heterotrophic denitrification were the primary N_2O emission pathways in the CANON process coupled with denitrification. These results were consistent with the thermodynamic prediction results in which the ΔG values of the nitrifier denitrification and heterotrophic denitrification were significantly greater than those of the NH_2OH oxidation, which was favorable for N_2O production (see Prediction of N_2O emission potential based on thermodynamics). The N_2O emissions produced by AOB were significantly higher than those produced by HD bacteria. In addition, the N_2O emissions by AOB via hydroxylamine oxidation comprised only approximately

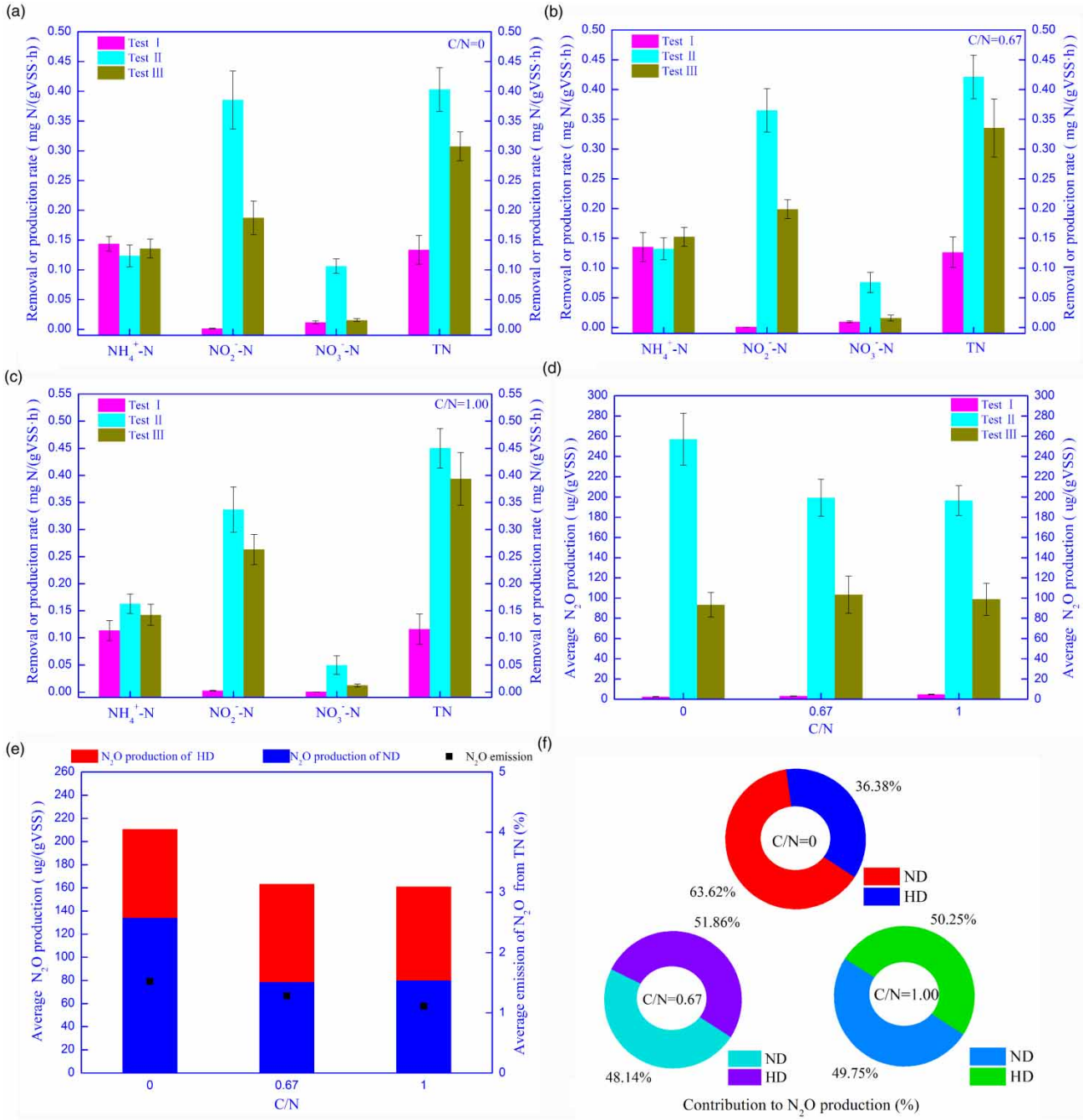

Figure 3 | Nitrogen transformation and emission characteristics of N_2O via nitrifier and heterotrophic nitrification during inhibition experiments with different C/N ratios: nitrogen transformation or removal using C/N ratios of 0 (a), 0.67 (b) and 1.00 (c), respectively; average N_2O production during inhibition experiments (d); average N_2O production via nitrifier and heterotrophic nitrification (e); and average contributions of nitrifier and heterotrophic nitrification to total N_2O production (f).

1/8 of the N_2O emissions by AOB via denitrification. With regard to N_2O emissions, AOB obtained a higher f_s^0 for substrate allocation via denitrification than that of NH_2OH oxidation. A higher f_s^0 is beneficial for the synthesis and growth of bacteria. Therefore, AOB preferred the denitrification pathway because of a growth advantage over NH_2OH oxidation in which N_2O needs to be produced by AOB. This hypothesis could explain why the N_2O emissions by AOB via denitrification were significantly higher than those produced by NH_2OH oxidation.

The spatial distributions of AOB, nitrite-oxidizing bacteria (NOB) and anammox bacteria in the biofilm were

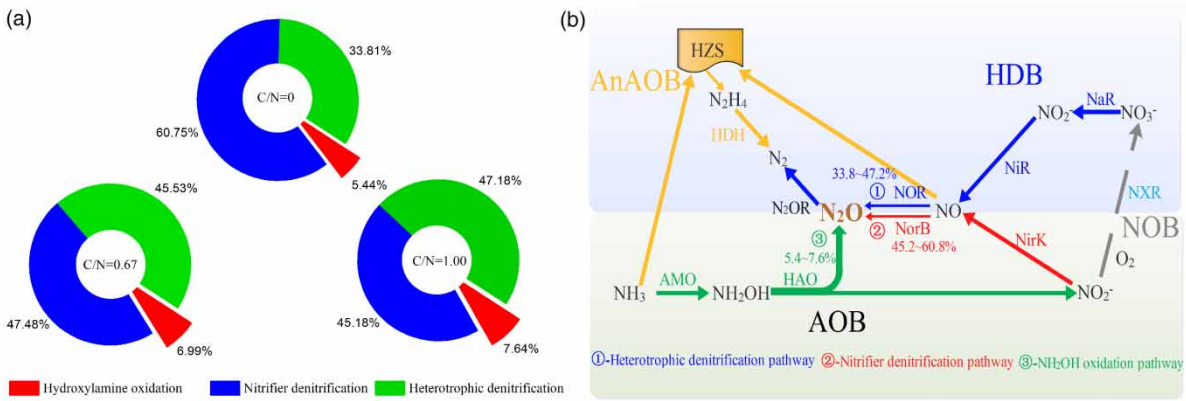

Figure 4 | Compositions (a) and pathways (b) of N_2O emissions in the SBBRs using different C/N ratios.

determined using FISH (Figure 5). NSO1225-stained AOB were detected primarily in the outermost surface layer of the biofilm, and the distribution of AOB was localized primarily in the surface layer of the biofilm (approximately 0–300 μm). GAM42a-T1038 and Pxyn-440-stained HD bacteria and Amx820-stained anammox bacteria cells were observed underneath the AOB cell layer. The distributions of anammox bacteria and HD bacteria were primarily localized at depths greater than 400 μm in the anaerobic microzone within the biofilm. In addition, the clearly

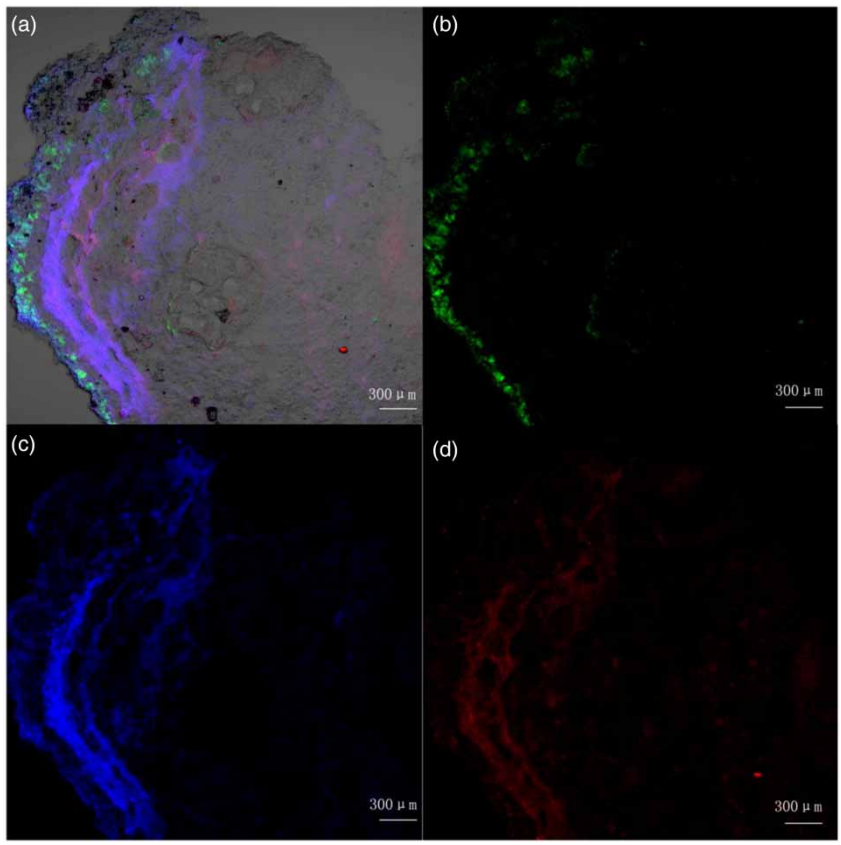

Figure 5 | Confocal laser scanning microscopy images of thin cross-sections of biofilm (a–d) from the SBBR with a C/N ratio of 0.67. These images show the *in situ* spatial organization of AOB (green), HD bacteria (blue) and anammox bacteria (red). Fluorescence *in situ* hybridization was performed with an FITC-labeled NSO1225 probe for AOB, Cy5-labeled GAM42a-T1038 and Pxyn-440 probes for HD bacteria and a Cy3-labeled AMX820 probe for anammox bacteria. The full colour version of this figure is available in the online version of this paper, at http://dx.doi.org/10.2166/wst.2020.344.

stratified spatial distributions of AOB and HD bacteria and anammox bacteria were observed. AOB and HD bacteria were the primary contributors to N_2O emissions. Therefore, the N_2O source region depended on the spatial distribution of aerobic AOB and HD bacteria.

The bacterial community structures in the three SBBRs are shown in Figure S5. *Thauera* and *Denitratisoma* were reported previously to be HD bacteria, and *Nitrosomonadaceae* and *Nitrosomonas* were reported previously to be AOB (Hu *et al.* 2010). The relative abundance of the genera of HD bacteria increased significantly from 3.4 to 12.8%, and the relative abundance of the AOB genera decreased from 5.9 to 3.6% as the C/N ratio increased. Although the relative abundance of HD bacteria significantly increased as the C/N ratio increased, heterotrophic denitrification N_2O emissions showed little change (see N_2O emissions via nitrifier and heterotrophic denitrification). This result indicated the carbon source had a limited effect on heterotrophic denitrification N_2O production. However, nitrifier denitrification N_2O production significantly decreased as the C/N ratio increased. Therefore, the inhibition of AOB by a carbon source effectively reduced N_2O production from nitrifier denitrification. N_2O emissions from nitrifier denitrification decreased as the C/N ratio increased, which was the main contributor to the reduction in the total N_2O emission in the process. The total N_2O emissions from TN decreased from 1.62 to 1.32% when the C/N ratio increased from 0 to 1 (see N_2O emissions via nitrification and denitrification with different C/N ratios). Therefore, the addition of an appropriate carbon source aids in the reduction of N_2O production from the CANON process coupled with denitrification.

CONCLUSION

N_2O emissions were investigated based on the thermodynamics and nitrogen transformation of a single-stage CANON process coupled with denitrification. The ΔG values of nitrifier denitrification and heterotrophic denitrification were significantly greater than that of NH_2OH oxidation, indicating nitrifier denitrification and heterotrophic denitrification were favorable for N_2O production. The value of f_s^0 in AOB denitrification was two times that of the NH_2OH oxidation during substrate allocation. Therefore, AOB preferred the denitrification pathway because of its growth advantage when N_2O was produced by the AOB. The N_2O emissions by hydroxylamine oxidation, nitrifier denitrification and heterotrophic denitrification in the SBBRs using different C/N ratios accounted for 5.4–7.6%, 45.2–60.8% and 33.8–47.2%, respectively, of the N_2O emissions. The total N_2O emissions from TN decreased from 1.62 to 1.32% when the C/N ratio increased from 0 to 1. The carbon source had no significant effect on the N_2O emission by NH_2OH oxidation and heterotrophic denitrification in this process. However, nitrifier denitrification N_2O production decreased significantly as the C/N ratio increased. The reduction in N_2O emissions by nitrifier denitrification was the primary contributor to reducing the total N_2O emissions in the process. The results of this study showed the addition of an appropriate carbon source aids in the reduction of N_2O production in the CANON process coupled with denitrification.

ACKNOWLEDGEMENTS

This work was supported by the National Natural Science Foundation of China (51878091 and 51278509), the Chongqing Science and Technology Bureau (cstc2018jcyjAX0610) and the Fundamental Research Funds for the Central Universities (2019CDQYCH036 and 2019CDXYCH0026).

DATA AVAILABILITY STATEMENT

All relevant data are included in the paper or its Supplementary Information.

REFERENCES

Ali, M., Rathnayake, R. M., Zhang, L., Ishii, S., Kindaichi, T., Satoh, H. & Okabe, S. 2016 Source identification of nitrous oxide emission pathways from a single-stage nitritation-anammox granular reactor. *Water Research* **102**, 147–157.

Castro-Barros, C. M., Daelman, M. R. J., Mampaey, K. E., van Loosdrecht, M. C. M. & Volcke, E. I. P. 2015 Effect of aeration regime on N_2O emission from partial nitritation-anammox in a full-scale granular sludge reactor. *Water Research* **68**, 793–803.

Chen, H., Liu, S., Yang, F., Xue, Y. & Wang, T. 2009 The development of simultaneous partial nitrification, ANAMMOX and denitrification (SNAD) process in a single reactor for nitrogen removal. *Bioresource Technology* **100** (4), 1548–1554.

Connan, R., Dabert, P., Moya-Espinosa, M., Bridoux, G., Beline, F. & Magrí, A. 2018 Coupling of partial nitritation and anammox in two- and one-stage systems: Process operation, N_2O emission and microbial community. *Journal of Cleaner Production* **203**, 559–573.

Desloover, J., Vlaeminck, S. E., Clauwaert, P., Verstraete, W. & Boon, N. 2012 Strategies to mitigate N_2O emissions from

biological nitrogen removal systems. *Current Opinion in Biotechnology* **23** (3), 474–482.

Domingo-Félez, C. & Smets, B. F. 2019 Regulation of key N_2O production mechanisms during biological water treatment. *Current Opinion in Biotechnology* **57**, 119–126.

Duan, H., Ye, L., Erler, D., Ni, B. J. & Yuan, Z. 2017 Quantifying nitrous oxide production pathways in wastewater treatment systems using isotope technology–a critical review. *Water Research* **122**, 96–113.

Hu, B., Zheng, P., Tang, C., Chen, J., van der Biezen, E., Zhang, L., Ni, B., Jetten, M. S. M., Yan, J., Yu, H. & Kartal, B. 2010 Identification and quantification of anammox bacteria in eight nitrogen removal reactors. *Water Research* **44**, 5014–5020.

Kampschreur, M. J., Poldermans, R., Kleerebezem, R., van der Star, W. R. L., Haarhuis, R., Abma, W. R., Jetten, M. S. M. & van Loosdrecht, M. C. M. 2009 Emission of nitrous oxide and nitric oxide from a full-scale single-stage nitritation-anammox reactor. *Water Science and Technology* **60**, 3211–3217.

Lackner, S., Gilbert, E. M., Vlaeminck, S. E., Joss, A., Horn, H. & van Loosdrecht, M. C. 2014 Full-scale partial nitritation/anammox experiences–an application survey. *Water Research* **55**, 292–303.

Law, Y., Lant, P. & Yuan, Z. G. 2011 The effect of pH on N_2O production under aerobic conditions in a partial nitritation system. *Water Research* **45** (18), 5934–5944.

Li, K., Fang, F., Wang, H., Wang, C., Chen, Y., Guo, J. S. & Jiang, F. 2017 Pathways of N removal and N_2O emission from a one-stage autotrophic N removal process under anaerobic conditions. *Scientific Reports* **7**, 42072.

Liang, Y., Li, D., Zhang, X., Zeng, H., Yang, Z. & Zhang, J. 2014 Microbial characteristics and nitrogen removal of simultaneous partial nitrification, anammox and denitrification (SNAD) process treating low C/N ratio sewage. *Bioresource Technology* **169**, 103–109.

Ma, C., Jensen, M. M., Smets, B. F. & Thamdrup, B. 2017 Pathways and controls of N_2O production in Nitritation–Anammox Biomass. *Environmental Science & Technology* **51** (16), 8981–8991.

Mannina, G., Ekama, G. A., Capodici, M., Cosenza, A., Di Trapani, D., Ødegaard, H. & Van Loosdrecht, M. M. 2018 Influence of carbon to nitrogen ratio on nitrous oxide emission in an Integrated Fixed Film Activated Sludge Membrane BioReactor plant. *Journal of Cleaner Production* **176**, 1078–1090.

McCarty, P. L. 2007 Thermodynamic electron equivalents model for bacterial yield prediction: modifications and comparative evaluations. *Biotechnology and Bioengineering* **97** (2), 377–388.

Okabe, S., Oshiki, M., Takahashi, Y. & Satoh, H. 2011 N_2O emission from a partial nitrification–anammox process and identification of a key biological process of N_2O emission from anammox granules. *Water Research* **45** (19), 6461–6470.

Peng, L., Ni, B. J., Ye, L. & Yuan, Z. G. 2015 The combined effect of dissolved oxygen and nitrite on N_2O production by ammonia oxidizing bacteria in an enriched nitrifying sludge. *Water Research* **73**, 29–36.

Rathnayake, R. M. L. D., Song, Y., Tumendelger, A., Oshiki, M., Ishii, S., Satoh, H., Toyoda, S., Yoshida, N. & Okabe, S. 2013 Source identification of nitrous oxide on autotrophic partial nitrification in a granular sludge reactor. *Water Research* **47** (19), 7078–7086.

Rittmann, B. E. & McCarty, P. L. 2012 *Environmental Biotechnology: Principles and Applications*. McGraw-Hill Higher Education, New York, NY, USA.

Sliekers, A. O., Derwort, N., Gomez, J. L., Strous, M., Kuenen, J. G. & Jetten, M. S. 2002 Completely autotrophic nitrogen removal over nitrite in one single reactor. *Water Research* **36** (10), 2475–2482.

Spinelli, M., Eusebi, A., Vasilaki, V., Katsou, E., Frison, N., Cingolani, D. & Fatone, F. 2018 Critical analyses of nitrous oxide emissions in a full scale activated sludge system treating low carbon-to-nitrogen ratio wastewater. *Journal of Cleaner Production* **190**, 517–524.

Tallec, G., Garnier, J., Billen, G. & Gousailles, M. 2008 Nitrous oxide emissions from denitrifying activated sludge of urban wastewater treatment plants, under anoxia and low oxygenation. *Bioresource Technology* **99**, 2200–2209.

Vázquez-Padín, J. R., Pozo, M. J., Jarpa, M., Figueroa, M., Franco, A., Mosquera-Corral, A., Campos, J. L. & Mendez, R. 2009 Treatment of anaerobic sludge digester effluents by the CANON process in an air pulsing SBR. *Journal of Hazardous Materials* **166** (1), 336–341.

Wang, X. X., Fang, F., Chen, Y. P., Guo, J. S., Li, K. & Wang, H. 2017 N_2O micro-profiles in biofilm from a one-stage autotrophic nitrogen removal system by microelectrode. *Chemosphere* **175**, 482–489.

Weissenbacher, N., Takacs, I., Murthy, S., Fuerhacker, M. & Wett, B. 2010 Gaseous nitrogen and carbon emissions from a full-scale deammonification plant. *Water Environment Research* **82**, 169–175.

Wrage, N., Velthof, G. L., Van Beusichem, M. L. & Oenema, O. 2001 Role of nitrifier denitrification in the production of nitrous oxide. *Soil Biology & Biochemistry* **33** (12), 1723–1732.

Yan, P., Li, K., Guo, J. S., Zhu, S. X., Wang, Z. K. & Fang, F. 2019 Toward N_2O emission reduction in a single-stage CANON coupled with denitrification: investigation on nitrite simultaneous production and consumption and nitrogen transformation. *Chemosphere* **228**, 485–494.

Zhang, X., Zhang, N., Wang, L., Zheng, K., Fu, H., Chen, T. & Yan, Y. 2017 Bioactivity and microbial community structure of nitrite-oxidizing bacteria in five membrane bioreactors operated as CANON process with different C/N ratio. *Ecological Engineering* **99**, 159–163.

First received 23 February 2020; accepted in revised form 16 July 2020. Available online 28 July 2020